IUST
Iran University of Science and Technology

Iranian Journal of Electrical and Electronic Engineering

Journal Homepage: ijeee.iust.ac.ir

Enhancing Load frequency control in power systems using Puma Optimizer – Proportional Integral Derivative Method

Trung Kien Do*, and Thanh Long Duong*(C.A.)

Abstract: Frequency instability is one of the causes of severe disturbances in the power system, including load shedding and widespread blackouts. Especially in modern power systems, frequency instability has even more serious consequences due to the propagation occurring in interconnected regions. Load frequency control (LFC) is a powerful tool in power system operation to ensure that the frequency is always within the allowable limits. The control parameters of LFC must be optimally adjusted for stable system operation. However, a suitable and robust method for optimal tuning of LFC control parameters is currently a challenge for researchers. The paper proposes the Puma Optimizer (PO) algorithm to optimize the parameters of PID, FOPID, and FOPTID+1 controllers for solving the LFC problem. The proposed PO algorithm is evaluated through two models of single-area and two-area power systems with different power sources, including thermal power, hydropower, and gas power. The simulation results show that the integral time absolute error (ITAE) value of the proposed PO method is smaller by 5.25%, 18.16%, 28.35%, and 59.92% compared to Particle Swarm Optimization (PSO), Crested Porcupine Optimization (CPO), Newton-Raphson-based optimization (NRBO), and Global Neighborhood Algorithm (GNA), respectively. The results obtained demonstrate that the PO algorithm is a reliable and efficient tool for finding solutions to the LFC problem.

Keywords: Load Frequency Control, Puma Optimizer, Meta-Heuristic, Power system.

1 Introduction

The uncertain and unpredictable nature of load demand may lead to an imbalance between load demand and generation power, thereby causing frequency deviations [1]. Furthermore, this problem increases in modern power systems with interconnected structures from multiple generation sources [2]. Frequency instability can not only lead to load shedding but also cause widespread power outages in severe cases [3]. This issue poses challenges for power system operators to regulate system frequency and tie-line power between areas within acceptable limits [4]. Load frequency control (LFC) is normally employed to solve these issues by adjusting generators' rotational speeds [5].

Over the years, a lot of work has been done by researchers in designing new control strategies for LFC. Many other types of controllers are also researched to improve control results, such as H-infinity control in [6], optimal control in [7], Intelligent Fuzzy TIDF-II Controller in [8], High Order Sliding Mode Control in [9], etc. However, the complex structure of the power system poses many challenges when applying these methods. Therefore, the structure of LFC is often based on conventional controllers, such as proportional-integral-derivative (PID) and its variants (PI, PD, I). These controllers are simple and easy to implement, so they are widely used in many studies, although their performance is limited [10]. To enhance control performance, a structured fractional order (FO)

Iranian Journal of Electrical & Electronic Engineering, YYYY.
Paper first received DD MONTH YYYY and accepted DD MONTH YYYY.
* Faculty of Electrical Engineering Technology, Industrial University of Ho Chi Minh City, Ho Chi Minh City, Viet Nam.
E-mails: dotrungkien731@gmail.com. (T. K. Do) and duongthanhlong@iuh.edu.vn (T.L. Duong).
Corresponding Author: T. L. Duong.

controller is proposed [11]. While this structure's inherent stability, robustness, and ability to eliminate uncertainty better than conventional controllers make it a promising alternative, the parameters of this controller need to be properly optimized to ensure the system's control performance [12]. A more complex controller called a cascade controller is used by the authors in [13, 14]. Its advantage is that there are a larger number of parameters than previous types of control, which improves performance significantly but takes more computational resources to tune.

Modern power systems are becoming increasingly complex with multiple controllers, which pose many challenges in determining suitable parameters for the controller in the LFC problem. Researchers often tune the controllers using two methods: gradient-based methods or metaheuristic optimization [15]. However, compared to classical gradient-based optimization methods, metaheuristics have advantages such as the ability to escape being stuck in local optima. This method has attracted considerable attention from researchers in the field of LFC. A typical example is in the literature [16], where the authors use Particle Swarm Optimization (PSO) and Genetic Algorithm (GA) techniques to tune the PID controller for both two-zone power systems and single-zone multi-source power networks. Similarly, the Honey Badger Algorithm (HBA) was chosen for tuning the PID controller by researchers in [17]. Another method used to tune the PID controller is proposed in [18], which is the Lyrebird Optimization Algorithm (LOA) technique. In paper [19], the researchers present the Sewing Training Based Optimization (STBO) method, a human-based meta-algorithm for optimizing the coefficients of the cascaded PI-PD controller. The FOPID-FOPI controller in [20] is tuned using a Chaotic Game Optimization (CGO) technique. In [21], the fractional order proportional tilt integral derivative plus one (FOPTID+1) controller is tuned by the Global Neighborhood Algorithm (GNA). The two-degree of freedom PID (2DOF PID) controller is optimized using the African Vulture Optimization Algorithm (AVOA) technique proposed in [22]. The tilt integral derivative (TID) controller is tuned using the Salp Swarm Algorithm (SSA) in [23]. This controller is optimized by the authors in [24] based on the hybrid Teaching-Learning and Pattern Search (hTLBO-PS) method.

Puma Optimizer (PO) is a new metaheuristic algorithm developed in 2024. The PO algorithm is inspired by the intelligence and hunting behavior of pumas. This algorithm provides a new approach to solving complex problems. From the above point of view, the PO algorithm is used in the study to optimize the tuning of PID, FOPID, and FOPTID+1 controllers to improve their performance for the LFC system. Two multi-source LFC systems, including a single-area LFC system model and a two-area LFC system model, are used to test the effectiveness of the PO algorithm. The sources in the system are thermal power, hydropower, and gas power. The simulation results are analyzed and evaluated, thereby validating the applicability of the proposed PO algorithm in adjusting controller parameters in the LFC problem. Furthermore, the results of the proposed method are compared with other state-of-the-art algorithms like PSO [25] and newly published algorithms such as the Crested Porcupine Optimization (CPO) algorithm [26] and the Newton-Raphson based Optimization (NRBO) algorithm [27], thereby highlighting the effectiveness of the proposed method over other methods.

The main contributions of this paper are summarized as follows:

- For the first time, the new meta-heuristic algorithm PO is applied to the controller design in the LFC system.
- Successfully implemented the PO method to find the optimal parameters of the PID, FOPID, and FOPTID+1 controllers.
- The results of the PO method are compared with state-of-the-art algorithms to demonstrate the effectiveness of the proposed method.
- The robustness of the controller tuned by the proposed method is confirmed by sensitivity analysis under large changes in critical system parameters.

The remainder of the paper is organized as follows: The mathematical model of the LFC systems is presented in Section 2. Section 3 introduces the controller structure and objective function of the LFC problem. Section 4 briefly introduces the algorithms and steps of applying the proposed method to solve the LFC problem. Section 5 demonstrates the effectiveness of the PO method by comparing the simulation results of the proposed method with those of other methods and analyzing the sensitivity of the controllers tuned by the proposed method. Finally, Section 6 presents the conclusions of this paper.

2 Modeling of LFC System

The power system is inherently highly complex and nonlinear [28]. Therefore, a linearized model of the load frequency control system is used for controller design purposes. This paper uses two LFC system models. The first model is the multi-source single area, and the second model is the multi-source two-area. The transfer function models of these are described in Fig. 1 and Fig. 2, respectively.

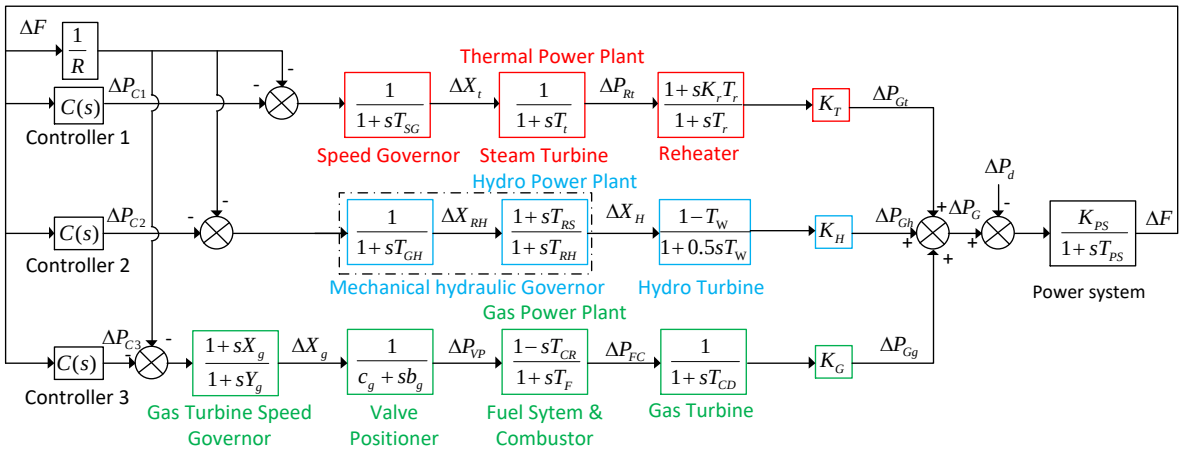

Fig. 1 Transfer function model of a multi-source single-area LFC system.

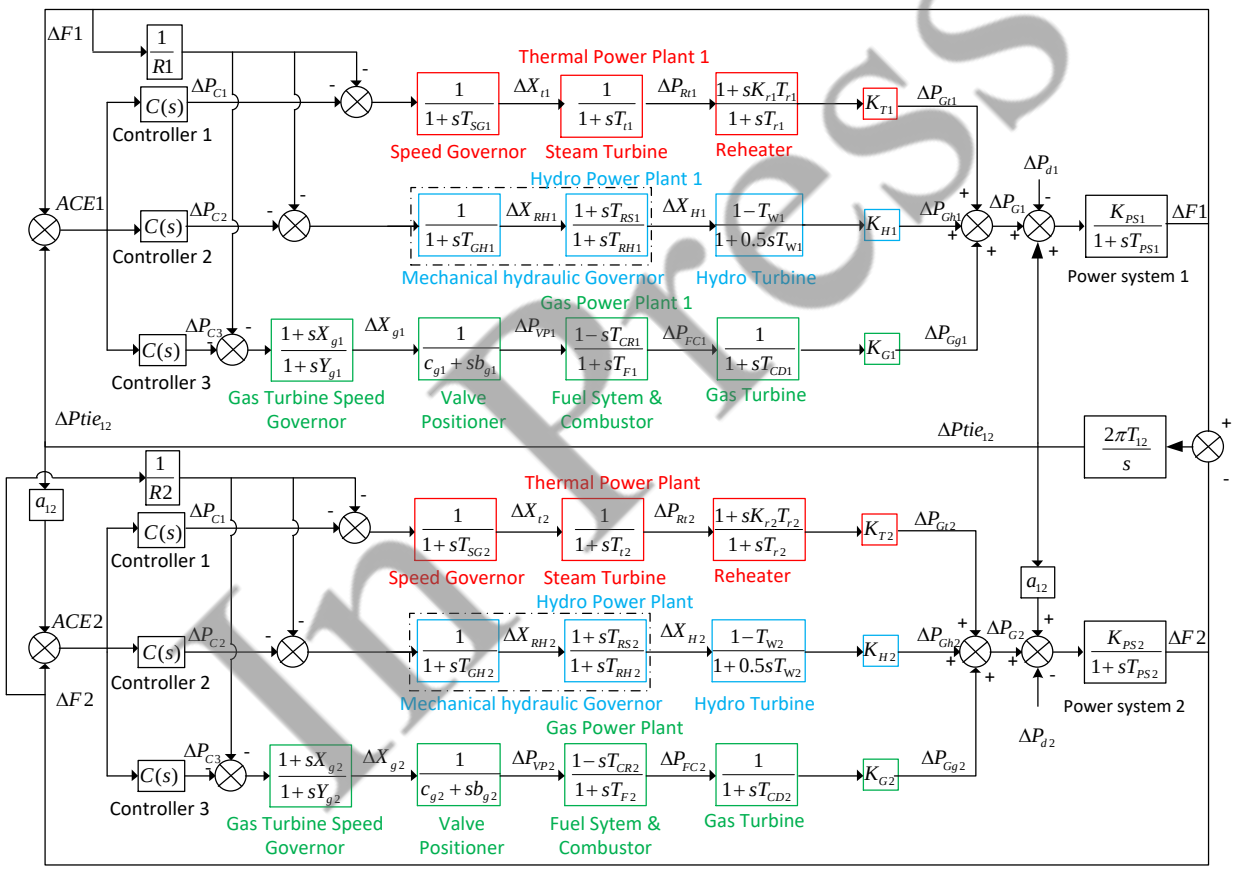

Fig. 2 Transfer function model of a multi-source two-area LFC system.

The sources include thermal, hydro, and gas. According to [29], the transfer functions of the generator/power system (G_{PS}) are given by Eq. (1).

$$G_{PS}(s) = \frac{K_{PS}}{1+sT_{PS}} \tag{1}$$

Where K_{PS} is the power system gain, T_{PS} is the power system time constant. The transfer functions of different components in thermal sources, such as the thermal speed governor (G_{TG}), steam turbine (G_{TT}), and reheat steam turbine (G_{TTr}), are denoted by Eq. (2), Eq. (3), and Eq. (4), respectively [29].

$$G_{TG}(s) = \frac{1}{1+sT_G} \tag{2}$$

$$G_{TT}(s) = \frac{1}{1+sT_T} \tag{3}$$

$$G_{TTr}(s) = \frac{1 + sK_r T_r}{1 + sT_r} \quad (4)$$

Where K_r is the reheat steam turbine gain. T_G, T_T, and T_r are the speed governor time constant, steam turbine time constant, and reheat steam turbine time constant, respectively. The transfer functions of different components in hydro sources are denoted by the hydro turbine (G_{HT}) and the mechanical hydraulic governor (G_{HT}), respectively, as per Eq. (5) and Eq. (6)[29].

$$G_{HT}(s) = \frac{1 - sT_W}{1 + 0.5sT_W} \quad (5)$$

$$G_{HG}(s) = \left[\frac{1}{1 + sT_{GH}}\right]\left[\frac{1 + sT_{RS}}{1 + sT_{RH}}\right] \quad (6)$$

Where T_W is the nominal starting time of water in the penstock, T_{GH} is the hydro turbine time constant, T_{RS} is the hydro turbine reset time constant, and T_{RH} is the hydro turbine transient droop time constant. The transfer functions of different components in gas sources are denoted by gas turbine (G_{TC}), fuel system with combustor (G_{FC}), valve positioner (G_{VP}), and gas governor (G_{GR}). They are given by Eq. (7), Eq. (8), Eq. (9), and Eq. (10), respectively [29].

$$G_{TC}(s) = \frac{1}{1 + sT_{CD}} \quad (7)$$

$$G_{FC}(s) = \frac{1 - sT_{CR}}{1 + sT_F} \quad (8)$$

$$G_{VP}(s) = \frac{1}{c_g + sb_g} \quad (9)$$

$$G_{GR}(s) = \frac{1 + sX_g}{1 + sY_g} \quad (10)$$

Where T_{CD} is the gas turbine compressor discharge volume time constant, T_{CR} is the gas turbine time delay, T_F is the hydro turbine reset time constant, c_g is the gas turbine valve positioner, b_g is the gas turbine constant of valve positioner, X_g is the lead time constant of gas turbine speed governor, Y_g is the lag time constant of gas turbine speed governor. The ACE1 and ACE2 are area control errors of Area 1 and Area 2 given by Eq. (11) and Eq. (12), respectively [29].

$$ACE_1 = \beta_1 \Delta F_1 + \Delta Ptie_{12} \quad (11)$$

$$ACE_2 = \beta_2 \Delta F_2 + \alpha_{12} \Delta Ptie_{12} \quad (12)$$

Where ΔF is the frequency variation, $\Delta Ptie_{12}$ is the change of tie-line power, β is the frequency bias parameter, a_{12} is the power transmission ratio between area-1 and area-2.

$$\Delta Ptie_{12} = \frac{2\pi T_{12}}{s}\left[\Delta F_1 - \Delta F_2\right] \quad (13)$$

Where T_{12} is the synchronizing torque coefficient between area-1 and area-2. The remaining parameters include: R is the regulating parameter of speed governor. K_T, K_H, and K_G are participation factors of thermal, hydro, and gas generating units, respectively. The simulations of the two models are performed via MATLAB 2016a.

3 Controller design

This paper uses three controller differences including PID, FOPID, and FOPTID+1. The PID controller is extremely popular in the field of control and automation due to its ease of design, tuning, and operation. According to [21, 30], the mathematical model of the PID controller is given by Eq. (14):

$$C(s) = K_P + \frac{K_I}{s} + sK_D \quad (14)$$

Where K_p, K_i và K_d are the proportional, integral, and derivative parameters of the controller, respectively.

The FOPID controller is an extension of the classic PID control paradigm by introducing non-integer orders for the proportional, integral, and derivative terms. According to [21], the mathematical model of the FOPID controller is given by Eq. (15):

$$C(s) = K_P + \frac{K_I}{s^\lambda} + s^\lambda K_D \quad (15)$$

If λ = μ = 1, FOPID will be a basic PID controller. The FOPTID+1 controller is similar to the FOPID controller but adds a parameter $K_T(s)^{1/n}$ and 1 to the control model. According to [21], the mathematical model of the FOPTID+1 controller is given by Eq. (16):

$$C(s) = K_P + \frac{K_T}{S^{1/n}} + \frac{K_I}{S^\lambda} + S^\lambda K_D + 1 \quad (16)$$

The low and upper boundaries of the parameters K_T, K_P, K_I, and K_D are [0-5]. The boundaries for λ and μ are [0-1], and for n, it is [1-3]. However, for the model of multi-source two areas, the range of KI is [0-6] for PID. The different performance indexes practiced in the LFC problem are integral absolute error (IAE), integral squared error (ISE), integral time squared error (ITSE), and integral time absolute error (ITAE). This paper uses an objective function expressed by Eq. (17) for the model of multi-source single areas and Eq. (18) for the model of multi-source two areas [21].

$$ITAE = \int_0^t t.|\Delta F|dt \quad (17)$$

$$ITAE = \int_0^t t.\left(|\Delta F_1| + |\Delta F_2| + |\Delta Ptie_{12}|\right)dt \quad (18)$$

Where t is the simulation time, Eq. (17) and Eq. (18) are used to optimize the parameters of the PID, FOPID, and FOPTID+1 controllers for the single-area LFC system model and the two-area LFC system model, respectively.

4 Proposed Method

4.1 Puma Optimization (proposed)

In this paper, a newly developed metaheuristic algorithm in 2024 by Abdollahzadeh and colleagues is applied to solve the LFC problem. The proposed method is built based on the intelligence and living behavior of pumas, a predator species commonly found on the American continent [31]. This section briefly presents the PO algorithm, including the exploration phase, exploitation phase, and phase transition mechanism.

In the wild, pumas often roam their large territories to patrol and hunt. They perform random searches within their territories or randomly approach other cougars' territories to find food. Inspired by this behavior, a mechanism for generating new solutions in the exploration phase of the PO algorithm is introduced as in Eq. (19) [31].

$$\begin{cases} \text{If } \text{rand}_1 > 0.5, Z_{i,G} = R_{Dim}.(Ub - Lb) + Lb \\ Otherwise \\ Z_{i,G} = X_{a,G} + G.\left(X_{a,G} - X_{b,G}\right) + G.\left(\left(X_{a,G} - X_{b,G}\right) - \left(X_{c,G} - X_{d,G}\right)\right) \\ \quad + G.\left(\left(X_{c,G} - X_{d,G}\right) - \left(X_{e,G} - X_{f,G}\right)\right) \end{cases} \quad (19)$$

Where $Z_{i,G}$ is the solution generated, Ub is the upper limit, Lb is the lower limit, R_{Dim} and $rand_1$ are random numbers from 0 to 1. $X_{a,G}$, $X_{b,G}$, $X_{c,G}$, $X_{d,G}$, $X_{e,G}$, and $X_{f,G}$ are the solutions in the entire population, which are randomly selected. G is the value calculated by the following Eq. (20).

$$G = 2.rand_2 - 1 \quad (20)$$

Where $rand_2$ is the random number from 0 to 1. Based on the conditions in Eq. (19), one of the two methods in Eq. (21) is selected to generate a new solution.

$$\begin{cases} \text{if } j = j_{rand} \text{ or } rand_3 \le U,\ X_{new} = Z_{i,G} \\ otherwise,\ X_{new} = X_{a,G} \end{cases} \quad (21)$$

Where, X_{new} is the new solution, j and j_{rand} are the current variables and randomly generated integers, respectively. $rand_3$ is the random number from 0 to 1. U is the fixed parameter set with a value from 0 to 1, which is updated by Eq. (22). This parameter ensures high diversity of selected solutions.

$$\begin{cases} if\ \text{CostX}_{new} < \text{CostX}_i,\ X_i = X_{new} \\ otherwise\ U = U + \dfrac{1-U}{N_{pop}} \end{cases} \quad (22)$$

Where CostX_i and CostX_{new} are the current cost and the new cost of the solution, respectively. X_i and $X_{i,new}$ are the current solution and the new solution, respectively. N_{pop} is the total number of Pumas.

In the exploitation phase of the PO algorithm, two operators are used to improve the solutions. These are inspired by two Puma hunting behaviors: ambush and sprinting, and these are described through Eq. (23) [31]. The operator simulating the sprinting characteristic of the Puma is used if $rand_4 \ge 0.5$. Otherwise, the Puma's ambush simulation operator will be selected. This operator consists of two different operations. The first operation simulates short jumps of the Puma towards other Pumas' hunts, and the second operation simulates the Puma's long jumps towards the best Puma's hunt.

$$\begin{cases} if\ rand_4 \ge 0.5 \\ X_{new} = \dfrac{\left(\dfrac{mean(Sol_{total})}{N_{pop}}\right).X_1^r - (-1)^{\beta}.X_i}{1 + (\alpha.rand_5)} \\ otherwise,\ if\ rand_6 \ge L, \\ X_{new} = Puma_{male} + (2.rand_7).\exp(randn_1).X_2^r - X_i \\ othewise \\ X_{new} = (2.rand_8).\dfrac{(F_1.R.X_i + F_2.(1-R).Puma_{male})}{(2.rand_9 - 1 + randn_2)} \\ \quad - Puma_{male} \end{cases} \quad (23)$$

$$if\ \text{CostX}_{new} < \text{CostX}_i,\ X_i = X_{new} \quad (24)$$

In Eq. (23), $rand_4$, $rand_5$, $rand_6$, $rand_7$, $rand_8$ and $rand_9$ are the random numbers. Their values are produced between 0 and 1. $randn_1$ and $randn_2$ are the randomly generated numbers from the normal distribution. Sol_{total} represents the sum of all solutions. Moreover, α and L are static parameters that must be tuned before the optimization procedure. β is a zero or one that is randomly produced. $Puma_{male}$ is the best solution. Also, the "$mean$" represents the mean function, and "exp" represents the exponential function. X_1^r is a randomly selected solution in the whole population. Finally, parameters X_2^r, R, F_1, and F_2 are calculated

using the equations that can be found in [31].

A phase change mechanism is proposed based on pumas' characteristics: very good memory and great intelligence. Based on this characteristic, the phase transition mechanism is divided into two stages: the early stage and the experienced stage. In the early stages of life, pumas do not have much experience, so they explore the territory and hunt at the same time. In this stage, the exploitation and exploration phases are performed simultaneously in the first three iterations. After the initial stage of life, pumas have the experience to optimize the decision of whether to explore new areas in the territory or hunt where prey often comes [31].

For the fourth iteration, the choice to enter the exploration and exploitation phase is made by calculating $Score_{Explore}$ and $Score_{Exploit}$ using the Eqs. (24-25). If $Score_{Explore}$ is greater than $Score_{Exploit}$, choose the exploration phase. Otherwise, choose the exploitation phase.

$$Score_{Explore} = \left(PF_1 . f_{1Explore}\right) + \left(PF_2 . f_{2Explore}\right) \quad (25)$$

$$Score_{Exploit} = \left(PF_1 . f_{1Exploit}\right) + \left(PF_2 . f_{2Exploit}\right) \quad (26)$$

In Eqs. (24-25), PF_1 and PF_2 are the fixed parameters set before the optimization process with values from 0 to 1. These are used to adjust the functions f_1 and f_2. The f_1 and f_2 are calculated using the equations that can be found in [31].

After each iteration in this stage, $Score^t_{Explore}$ and $Score^t_{Exploit}$ are calculated to choose the exploration or exploitation phase in the next iteration, which are calculated using Eqs. (26-27). If $Score^t_{Explore}$ is greater than $Score^t_{Exploit}$, choose the exploration phase. Otherwise, choose the exploitation phase.

$$\begin{aligned} Score^t_{Explore} = &\left(\alpha^t_{Explore} . f^t_{1Explore}\right) + \left(\alpha^t_{Explore} . f^t_{2Explore}\right) \\ &+ \left(\delta^t_{Explore} . \left(lc . f^t_{3Explore}\right)\right) \end{aligned} \quad (27)$$

$$\begin{aligned} Score^t_{Exploit} = &\left(\alpha^t_{Exploit} . f^t_{1Exploit}\right) + \left(\alpha^t_{Exploit} . f^t_{2Exploit}\right) \\ &+ \left(\delta^t_{Exploit} . \left(lc . f^t_{3Exploit}\right)\right) \end{aligned} \quad (28)$$

In Eqs. (26-27), t represents the present iteration number. Parameters α, f_1, f_2, f_3, lc, and δ are calculated using the equations that can be found in [31]. Similar to parameters PF1 and PF2 used to adjust functions f_1 and f_2, function f_3 also uses parameter PF3. This parameter is a fixed value selected before the optimization process and can range from 0 to 1.

4.2 The application of the PO algorithm to solve LFC problem

In this study, the LFC problem is solved using the PO algorithm. Details of the application of PO are presented through the following steps:

Step 1: Modeling the LFC system and controller using Eqs. (1-16). Input solution size (Dim), population size (N_{pop}), max iterations (IterMax), and the control parameters of the PO algorithm from Table 1. Create initial population (X_0) including solutions that are controller parameters created randomly by Eq. (29).

$$X_0^j = R_{Dim} . \left(Ub - Lb\right) + Lb, j = 1, ...N_{pop} \quad (29)$$

Where X_0^i is the j-th solution of the initial population. Ub and Lb are the upper limit and the lower limit of controller parameters, which are determined by Eq. (30).

$$\begin{cases} Lb = \left[K_T^{\min}, n^{\min}, K_P^{\min}, K_I^{\min}, K_D^{\min}, \lambda^{\min}, \mu^{\min}\right] \\ Ub = \left[K_T^{\max}, n^{\max}, K_P^{\max}, K_I^{\max}, K_D^{\max}, \lambda^{\max}, \mu^{\max}\right] \end{cases} \quad (30)$$

Step 2: Run the LFC system with each solution and calculate the objective function (ITAE) using Eqs. (17-18). Point out the best solution ($Puma_{male}$) and its ITAE value (Cost$Puma_{male}$).

Step 3: Apply the Exploration phase to create a new population (X_{new}) using Eqs. (19-21). Run the LFC system with each solution and calculate the ITAE value using Eqs. (17-18). Update the population of the Exploration phase ($X_i^{Explora}$) using Eq. (31).

$$\begin{cases} if\ \text{Cost}X_{new} < \text{Cost}X_i,\ X_i^{Explora} = X_{new} \\ otherwise\ U = U + \dfrac{1-U}{N_{pop}} \end{cases} \quad (31)$$

Step 4: Apply the Exploitation phase to create a new population (X_{new}) using Eq. (23). Run the LFC system with each solution and calculate the ITAE value using Eqs. (17-18). Update the population of the Exploitation phase ($X_i^{Exploit}$) using Eq. (32).

$$if\ \text{Cost}X_{new} < \text{Cost}X_i,\ X_i^{Exploit} = X_{new} \quad (32)$$

Step 5: Sort the solutions of (X_{i-1}, $X_i^{Explora}$, and $X_i^{Exploit}$) from smallest to largest based on their ITAE value. Update the population (X_i) based on the smallest solutions that are equal to the population size (N_{pop}). Update the best solution ($Puma_{male}$) and their ITAE value (Cost$Puma_{male}$) using Eq. (33).

$$\begin{aligned} &if\ \text{Cost}X_i^{Best} < \text{Cost}Puma_{male}, \\ &Puma_{male} = X_i^{Best} \\ &\text{Cost}Puma_{male} = \text{Cost}X_i^{Best} \end{aligned} \quad (33)$$

Where X_i^{Best} the best controller parameters and $\text{Cost}X_i^{Best}$ is its ITAE value in the i-th iteration.

Step 6: If iteration < 3, then increase iteration by 1 unit and return to Step 3; else go to Step 7.

Step 7: Calculate $Score_{Explore}$ and $Score_{Exploit}$ using Eqs. (25-26).

Step 8: If $Score_{Explore} > Score_{Exploit}$, apply the Exploration phase to create a new population (X_{new}) using Eqs. (19-21). Run the LFC system with each solution and calculate the ITAE value using Eqs. (17-18). Update the population (X_i) using Eq. (22); else apply the Exploitation phase to create a new population (X_{new}) using Eq. (23). Run the LFC system with each solution and calculate the ITAE value using Eqs. (17-18). Update the population (X_i) using Eq. (24).

Step 9: Update best solutions ($Puma_{male}$) and their ITAE value ($\text{Cost}Puma_{male}$) using Eq. (33).

Step 10: If iteration < IterMax then calculate $Score_{Explore}$ and $Score_{Exploit}$ using Eqs. (27-28) and return to Step 8; else print out the best controller parameters ($Puma_{male}$) and stop the program.

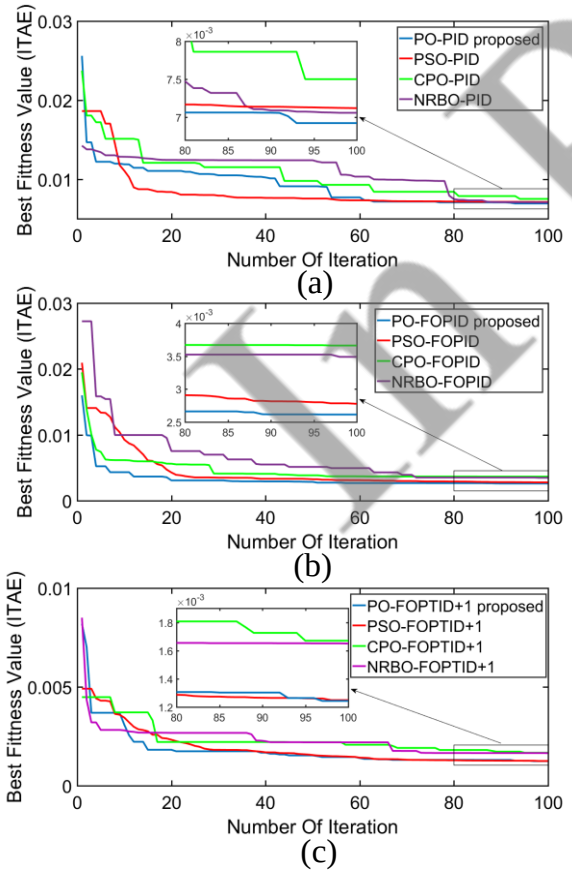

Fig. 3 Convergence curve of algorithms: (a) tuned PID (b) tuned FOPID (c) tuned FOPTID+1.

5 Simulation Results

In this study, the parameters of the proposed PO algorithm are shown in [31]. In order to demonstrate the effectiveness of the PO algorithm compared to PSO, CPO, and NRBO algorithms, the initial parameters of the algorithms are used the same, with 20 solutions and 100 iterations.

5.1 Model of LFC single-area

The parameters of the model of LFC single-area can be seen in [21, 29]. The controller parameters are tuned by optimization algorithms with a load disturbance at t=0 (sec), decreasing 1% total load ($\Delta Pd = -0.01$ p.u.MW). The convergence curves of the algorithms when tuning parameters for the PID, FOPID, and FOPTID+1 controllers are depicted in Fig. 3. Fig. 4 presents the frequency deviation of PID, FOPID, and FOPTID+1 controllers in the LFC system. The values of ITAE, settling time (S.T), overshoot (O.S), and undershoot (U.S) are computed and presented in Table 1 with the controller parameters optimized by the algorithms. The controller parameters optimized by the proposed algorithms are presented in Table 3.

The observation results in Fig. 3 and Table 1 show that

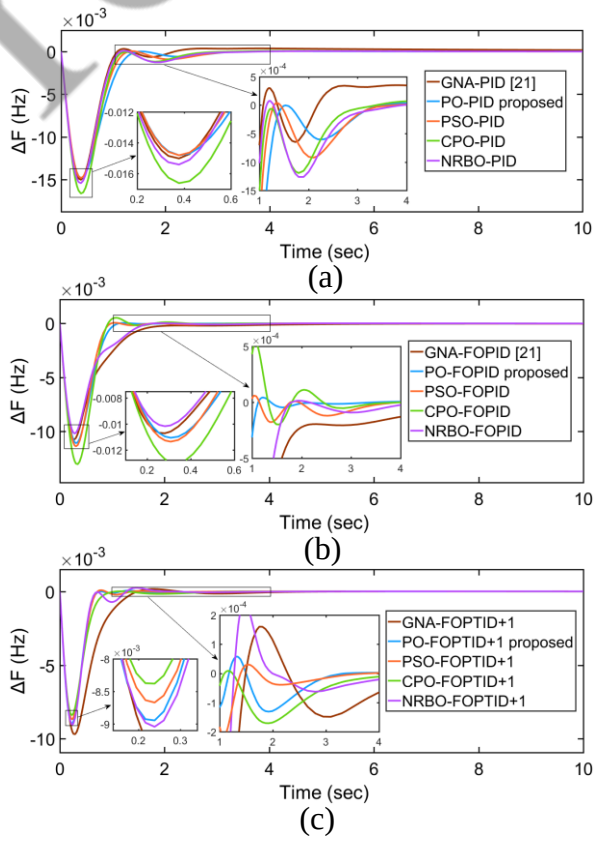

Fig. 4 Change in frequency for 1% step load perturbation: (a) using PID (b) using FOPID (c) using FOPTID+1.

the ITAE values of PID, FOPID, and FOPTID +1 controllers tuned by PO are 0.00692, 0.002613, and 0.001237, respectively, which are smaller than GNA by 0.01569 (55.9%), 0.00652 (59.92%), and 0.003435 (63.84%), respectively; PSO by 0.007122 (2.84%), 0.002758 (5.25%), and 0.001242 (0.04%), respectively; CPO by 0.007501 (7.75%), 0.003193 (18.16%), and 0.001669 (25.88%), respectively; and NRBO by 0.007085 (2.33%), 0.003647 (28.35%), and 0.001621 (23.69%), respectively. In addition, the results in Fig. 4 and the parameters in Table 1 show that the values S.T of PO are the least. This is the main reason that although in some cases the PO method has O.S. and U.S. larger than other methods, the ITAE value of PO is still the smallest. Through the above evaluations, the effectiveness of the proposed method has been confirmed.

5.2 Model of LFC two-area

The parameters of the model of LFC two-area can be seen in [21, 26]. With a load disturbance of 1% (ΔPd = 0,01 p.u.MW) at t = 0 (sec) in Area 1, the controller parameters optimized by the proposed algorithms are presented in Table 3. The convergence curves of the algorithms when tuning parameters for the PID, FOPID, and FOPTID+1 controllers are depicted in Fig. 5. Fig. 6, Fig. 7, and Fig. 8 present the frequency deviation in Area 1, Area 2, and tie-line power deviation of the PID, FOPID, and FOPTID+1 controllers in a two-area LFC system, respectively. The values of ITAE, S.T, O.S, and U.S are computed and presented in Table 2 with the controller parameters optimized by the algorithms.

The observation results in Fig. 5 and Table 2 show that the ITAE values of PID, FOPID, and FOPTID +1 controllers tuned by PO are 0.03531, 0.0197, and 0.01082, respectively, which are smaller than GNA by 0.04725 (25.27%), 0.04527 (56.48%), and 0.02180 (50.36%), respectively; PSO by 0.03678 (4%), 0.02047 (3.76%), and 0.01122 (3.57%), respectively; CPO by 0.03778 (6.54%), 0.02277 (13.48%), and 0.01321 (25.88%), respectively; and NRBO by 0.03649 (3.23%), 0.02053 (4.04%), and 0.01231 (12.1%), respectively. In addition, the observation results in Fig. 6, Fig. 7, and Fig. 8 show that the frequency deviation in Areas 1 and 2, as well as the tie-line power deviation values of the controllers optimized by the PO method, return to zero most quickly. Therefore, the S.T value of the PO method in Table 2 is the smallest. This leads to results similar to the case in the LFC single area. Although the values O.S and U.S of PO are not smaller than those of other methods in all cases, the ITAE of the proposed method is still the smallest. Through the above evaluations, the effectiveness of the proposed method has been confirmed once more.

Table 1 Performance indices of the dynamic responses corresponding to various controllers in the single-area LFC system.

Controller	Algorithm	ITAE	S. T (ses)	O.S	U.S
PID	GNA [21]	0.015690	12	0.000362	0.015020
	PO	0.006920	3.2	0.000034	0.014790
	PSO	0.007122	3.2	0.000061	0.014800
	CPO	0.007501	3.2	0.000076	0.016580
	NRBO	0.007085	3.4	0.000083	0.015400
FOPID	GNA [21]	0.006520	5.9	0.000000	0.010730
	PO	0.002613	3.1	0.000427	0.011080
	PSO	0.002758	3.6	0.000060	0.011370
	CPO	0.003193	3.6	0.000524	0.013030
	NRBO	0.003647	4.5	0.000014	0.010180
FOPTID+1	GNA [21]	0.003435	6.3	0.000016	0.009687
	PO	0.001237	3.2	0.000058	0.008947
	PSO	0.001242	3.5	0.000083	0.008672
	CPO	0.001669	4.8	0.000008	0.008381
	NRBO	0.001621	5.6	0.000246	0.009044

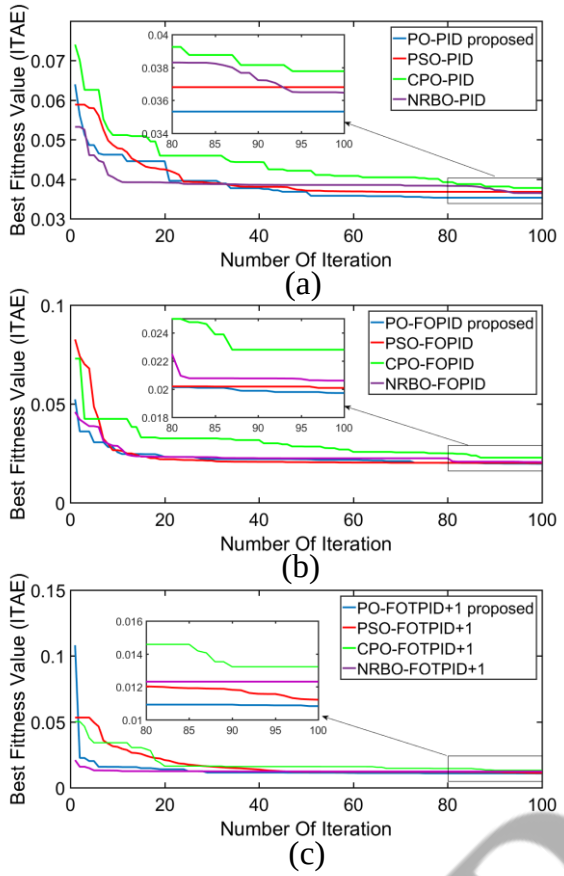

Fig. 5 Convergence curve of algorithms: (a) tuned PID (b) tuned FOPID (c) tuned FOPTID+1.

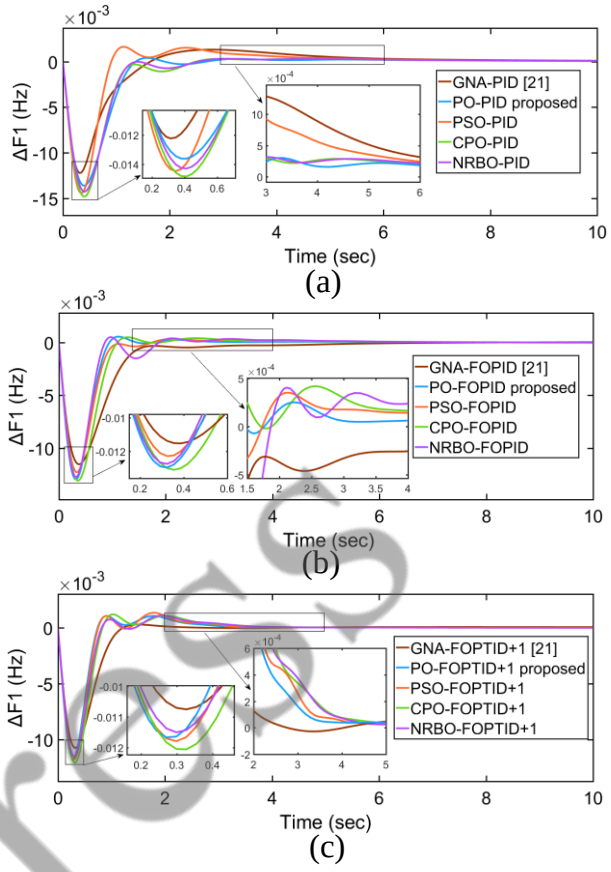

Fig. 6 Change in frequency of area-1 for 1% step load perturbation in area-1: (a) using PID (b) using FOPID (c) using FOPTID+1.

Table 2 Performance indices of the dynamic responses corresponding to various controllers in the two-area LFC system.

Method	ITAE	S. T (ses)			O.S			U.S		
		$\Delta F1$	$\Delta F2$	ΔP_{tie}	$\Delta F1$	$\Delta F2$	ΔP_{tie}	$\Delta F1$	$\Delta F2$	ΔP_{tie}
GNA-PID	0.04725	7.2	18	16	0.00131	0.00038	0.00012	0.0122	0.0050	0.0014
PO-PID	0.03531	5.8	6.5	8.2	0.00040	0.00004	0.00002	0.0136	0.0066	0.0018
PSO-PID	0.03678	6.5	16	14	0.00162	0.00022	0.00011	0.0145	0.0062	0.0016
CPO-PID	0.03778	6.0	6.5	8.2	0.00029	0.00003	0.00001	0.0148	0.0071	0.0019
NRBO-PID	0.03649	6.2	6.5	8.5	0.00000	0.00004	0.00001	0.2890	0.0068	0.0019
GNA-FOPID	0.04527	6.5	7.5	12	0.00004	0.00000	0.00000	0.0115	0.0054	0.0016
PO-FOPID	0.01970	4.9	7.6	7.5	0.00056	0.00000	0.00000	0.0130	0.0052	0.0014
PSO-FOPID	0.02047	5.7	6.8	6.9	0.00035	0.00000	0.00000	0.0123	0.0049	0.0014
CPO-FOPID	0.02277	5.7	7.2	7.3	0.00005	0.00000	0.00000	0.0131	0.0057	0.0016
NRBO-FOPID	0.02053	5.9	6.0	7.0	0.00052	0.00000	0.00000	0.0128	0.0050	0.0013
GNA-FOPTID+1	0.02180	2.5	7.6	8.8	0.00029	0.0000	0.00000	0.0108	0.0043	0.0013
PO-FOPTID+1	0.01082	3.5	5.3	5.5	0.00107	0.00000	0.00000	0.0117	0.0041	0.0011
PSO- FOPTID+1	0.01122	4.1	5.2	5.5	0.00134	0.00006	0.00000	0.0118	0.0042	0.0012
CPO- FOPTID+1	0.01321	4.7	5.3	5.5	0.00197	0.00000	0.00000	0.0121	0.0046	0.0013
NRBO- FOPTID +1	0.01231	5.4	5.4	5.5	0.00109	0.00000	0.00000	0.0115	0.0042	0.0012

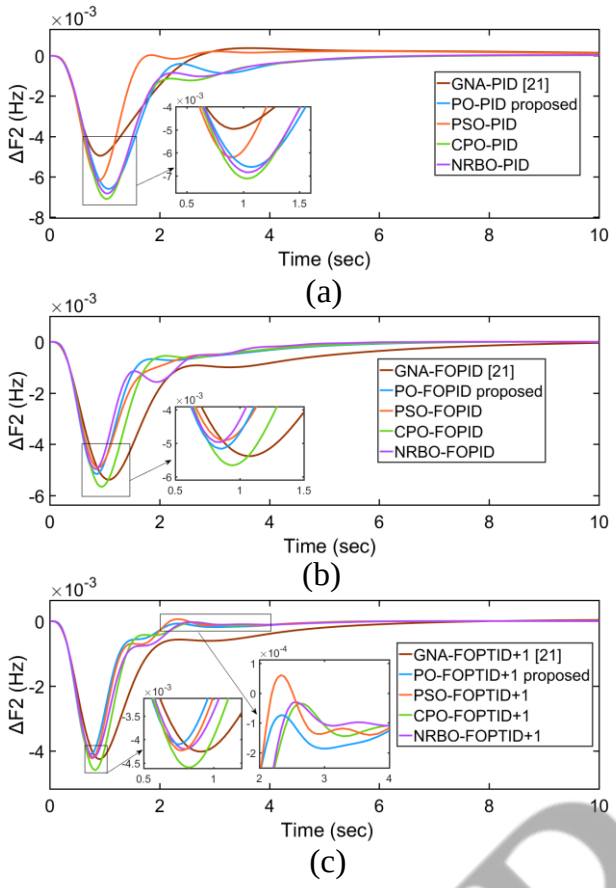

Fig. 7 Change in frequency of area-2 for 1% step load perturbation in area-1: (a) using PID (b) using FOPID (c) using FOPTID+1.

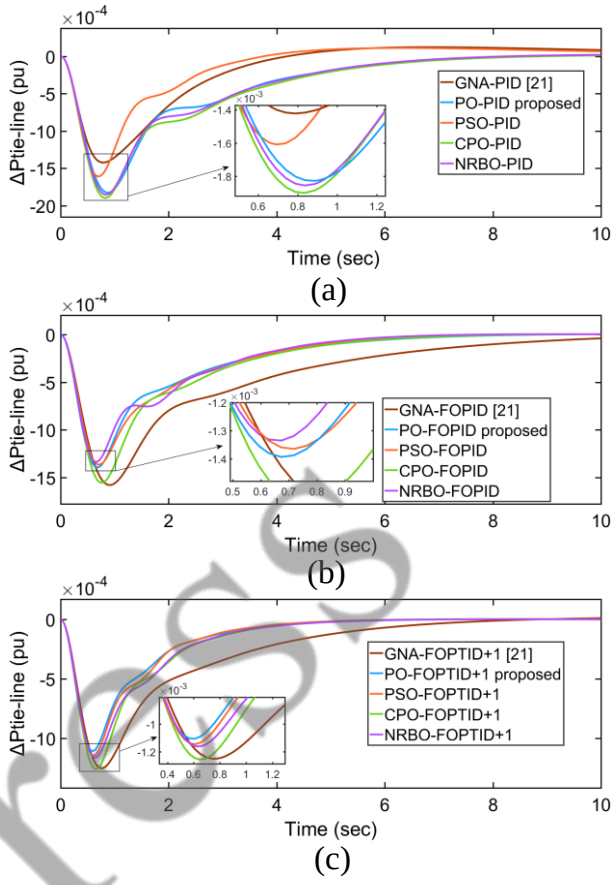

Fig. 8 Change in tie line power deviation for 1% step load perturbation in area-1: (a) using PID (b) using FOPID (c) using FOPTID+1.

Table 3 The parameters of the controllers are optimized using the proposed algorithm.

System	Parameter	i	K_{Ti}	N_i	K_{Pi}	K_{Ii}	K_{Di}	λ_i	μ_i
Single area	PID	1	-	-	5.0000	0.0048	1.9046	-	-
		2	-	-	5.0000	1.3893	0.7280	-	-
		3	-	-	0.0594	5.0000	0.0031	-	-
	FOPID	1	-	-	4.9746	4.9829	3.1882	0.6067	0.7833
		2	-	-	1.0686	5.0000	1.5144	0.7507	0.2922
		3	-	-	0.8053	4.5940	0.0051	0.9805	0.0001
	FOPTID+1	1	4.5408	2.9958	4.4416	4.9994	4.5872	0.5667	0.9908
		2	4.7040	2.9581	4.4607	4.9912	4.6257	0.9826	0.5656
		3	4.9563	1.0653	0.1532	4.9845	2.4095	0.9868	0.9810
Two-area	PID	1	-	-	4.9996	1.1269	3.7340	-	-
		2	-	-	5.0000	0.0000	0.8271	-	-
		3	-	-	4.9787	6.0000	0.0115	-	-
	FOPID	1	-	-	4.9996	4.9998	4.9652	0.7151	0.9997
		2	-	-	4.9958	5.0000	2.4941	0.6237	1.0000
		3	-	-	4.7339	5.0000	4.4390	1.0000	0.0012
	FOPTID+1	1	4.9878	1.7959	4.9992	5.0000	4.9996	0.7613	1.0000
		2	4.9992	1.6159	0.0012	4.9312	2.4785	0.6041	0.9995
		3	4.9985	1.2321	4.4995	4.9928	4.4574	0.9978	0.4333

Table 4 Statistical results obtained across different algorithms.

System	Method	Computation time (sec)	Min	Average	Max	Standard Deviation
Single-area	PO-PID	613	0.00692	0.00768	0.00896	0.00067
	PSO-PID	587	0.00712	0.01054	0.01142	0.00130
	CPO-PID	858	0.00750	0.00870	0.00954	0.00072
	NRBO-PID	563	0.00706	0.00787	0.00839	0.00061
	PO-FOPID	2558	0.00261	0.00311	0.00359	0.00034
	PSO-FOPID	2413	0.00277	0.00302	0.00359	0.00023
	CPO- FOPID	2955	0.00366	0.00447	0.00570	0.00056
	NRBO- FOPID	2343	0.00349	0.00378	0.00439	0.00026
	PO-FOPTID+1	3427	0.00124	0.00136	0.00152	0.00013
	PSO-FOPTID+1	2913	0.00125	0.00137	0.00165	0.00017
	CPO-FOPTID+1	4266	0.00165	0.00208	0.00246	0.00024
	NRBO-FOPTID+1	2871	0.00167	0.00188	0.00212	0.00017
Two-area	PO-PID	903	0.03532	0.0367	0.03790	0.00071
	PSO-PID	876	0.03680	0.0372	0.03768	0.00023
	CPO-PID	1340	0.03777	0.0388	0.04022	0.00065
	NRBO-PID	865	0.03665	0.0381	0.04218	0.00193
	PO-FOPID	4173	0.01972	0.0207	0.02184	0.00068
	PSO-FOPID	4065	0.02008	0.0211	0.02205	0.00069
	CPO- FOPID	6225	0.02279	0.0239	0.02495	0.00064
	NRBO- FOPID	4264	0.0206	0.0247	0.00359	0.00363
	PO-FOPTID+1	5460	0.01082	0.0115	0.01281	0.00055
	PSO-FOPTID+1	5214	0.01121	0.0125	0.01408	0.00108
	CPO-FOPTID+1	7988	0.01321	0.0145	0.01485	0.00076
	NRBO-FOPTID+1	5557	0.01231	0.0161	0.02475	0.00404

5.3 Sensitivity, robustness and stability analysis

This section examines the sensitivity, robustness, and stability of the PO method when applied to the LFC problem through analysis. Fig. 9 is a box plot depicting the distribution of ITAE values achieved by the PID controller in a single-area LFC system. These values were obtained through 20 runs of each algorithm. This analysis is intended to evaluate the performance and robustness of the proposed algorithm compared to other algorithms by providing insights into the variability and consistency of their performance. The results in Fig. 9 show that PO exhibits a narrower range of ITAE values, indicating its robustness and reliability compared to the other algorithms. The results for other scenarios were analogous. Table 4 is presented to provide comprehensive statistics of the results obtained from the various algorithms. This table presents a summary of key performance metrics, including computation time, minimum, maximum, average, and standard deviation ITAE values. Table 4 shows that PO has a higher computation time than most of the other algorithms, except CPO. However, considering the superior performance in the remaining metrics, this is acceptable.

Additionally, a sensitivity analysis was conducted for the single-area LFC system equipped with a PID controller as a representative case for the remaining cases. This analysis considered scenarios in which parameters T_G, T_T, T_r, T_{GH}, T_W, and T_{CD} were perturbed by ± 25% from their nominal values while maintaining the previously obtained optimal controller parameters. Table 5 and Table 6 present the performance indices of the PID controller in the single-area LFC model and the FOPTID+1 controller in the two-area LFC model, respectively. These controllers were optimized by the proposed method and considered under different variation conditions of the critical parameters.

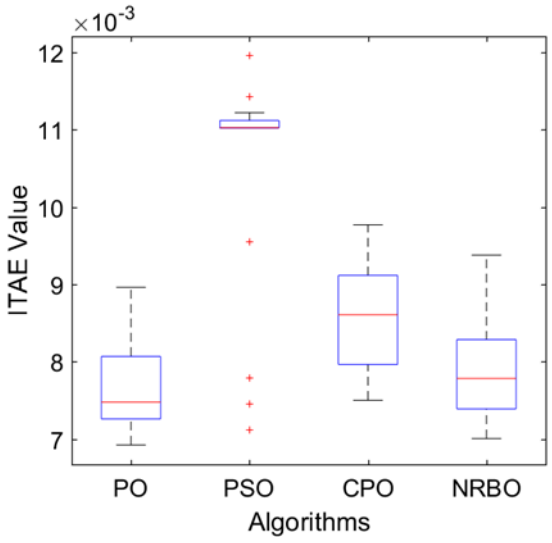

Fig. 9 Boxplot analysis of the PO, PSO, CPO, and NRBO algorithms.

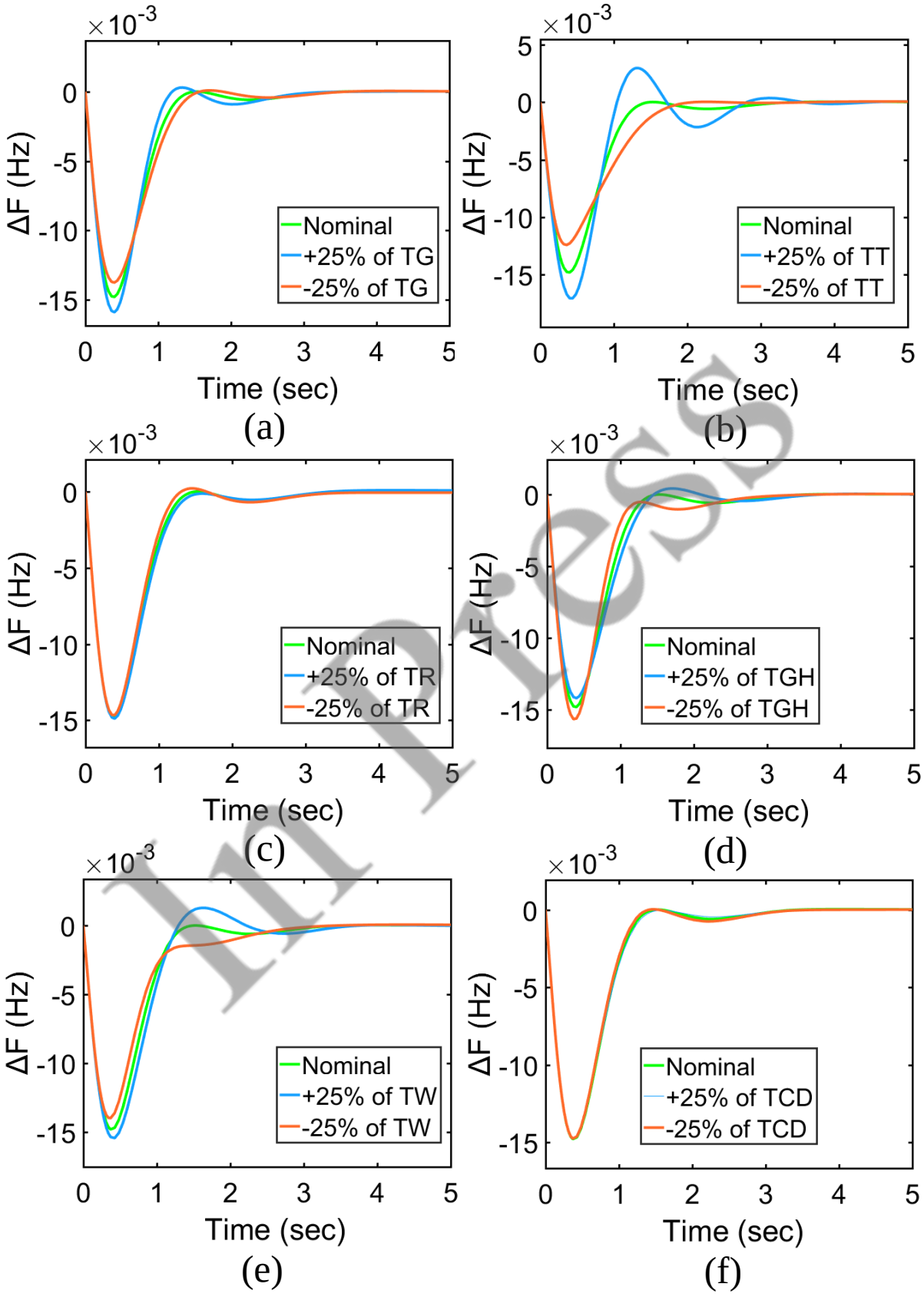

Fig. 10 Change in frequency for 1% step load perturbation with ± 25% change in: (a) T_G , (b) T_T , (c) T_r , (d) T_{GH} , (e) T_W , (f) T_{CD} .

Table 5 Performance indices of the dynamic responses corresponding to system parameter variations. (PID controller tuned by PO in single-area LFC system).

Parameter	Change (%)	ITAE	S. T (ses)	O.S	U.S
Nominal	0	0.006893	3.2	0.000034	- 0.01480
T_G	+ 25	0.006848	3.2	0.000298	- 0.01590
	- 25	0.007129	3.2	0.000094	- 0.01376
T_T	+ 25	0.010930	4.5	0.002969	- 0.01704
	- 25	0.073090	2.0	0.000053	- 0.01241
T_R	+ 25	0.008773	3.2	0.000093	- 0.01488
	- 25	0.008718	3.2	0.000218	- 0.01466
T_{GH}	+ 25	0.007390	3.5	0.000425	- 0.01418
	- 25	0.007048	3.0	0.000040	- 0.01450
T_W	+ 25	0.008599	3.8	0.001291	- 0.01545
	- 25	0.008234	3.2	0.000075	- 0.01399
T_{CD}	+ 25	0.069520	3.2	0.000063	- 0.01483
	- 25	0.006889	3.2	0.000023	- 0.01476

Table 6 Performance indices of the dynamic responses corresponding to system parameter variations. (FOPTID+1 controller tuned by PO in two-area LFC system).

Parameter	Change (%)	ITAE	S. T (sec)			O.S			U.S		
			$\Delta F1$	$\Delta F2$	ΔP_{tie}	$\Delta F1$	$\Delta F2$	ΔP_{tie}	$\Delta F1$	$\Delta F2$	ΔP_{tie}
Nominal	0	0.01082	3.5	5.3	5.5	0.00107	0.00000	0.00000	0.0117	0.0041	0.0011
T_{GT}	+25	0.01103	3.5	5.3	5.5	0.00209	0.00000	0.00000	0.0125	0.0043	0.0012
	-25	0.01099	3.5	5.3	5.5	0.00094	0.00000	0.00000	0.0108	0.0039	0.0011
T_T	+25	0.01273	3.5	5.3	5.5	0.00357	0.00004	0.00000	0.0131	0.0046	0.0013
	-25	0.01119	3.5	5.3	5.5	0.00106	0.00000	0.00000	0.0101	0.0036	0.0010
T_R	+25	0.01162	4.6	5.3	5.5	0.00100	0.00000	0.00000	0.0117	0.0041	0.0011
	-25	0.01073	3.5	5.3	5.5	0.00128	0.00000	0.00000	0.0116	0.0040	0.0011
T_{GH}	+25	0.01100	3.5	5.3	5.5	0.00103	0.00000	0.00000	0.0113	0.0041	0.0011
	-25	0.01072	3.5	5.3	5.5	0.00120	0.00000	0.00000	0.0123	0.0041	0.0011
T_W	+25	0.01095	3.5	5.3	5.5	0.00133	0.00000	0.00000	0.0120	0.0043	0.0012
	-25	0.01072	3.5	5.3	5.5	0.00095	0.00000	0.00000	0.0113	0.0039	0.0010
T_{CD}	+25	0.01096	3.5	5.3	5.5	0.00118	0.00000	0.00000	0.0118	0.0042	0.0011
	-25	0.01072	3.5	5.3	5.5	0.00109	0.00000	0.00000	0.0116	0.0040	0.0011

6 Conclusions

In this paper, the PO algorithm is proposed to optimize the parameters of PID, FOPID, and FOPTID+1 controllers. These controllers are used to control the frequency of both single-area and two-area LFC systems. These systems are simulated in MATLAB/Simulink to consider the frequency and tie line power variations with load changes. The obtained ITAE value shows that the results of the proposed PO method at the single-area and two-area models are smaller than PSO by 5.25% and 3.76%, respectively; CPO by 18.16% and 13.48%, respectively; NRBO by 28.35% and 4.04%, respectively; and GNA by 59.92% and 56.48%, respectively, when using the FOPID controller. Additionally, the controllers maintain efficiency even when critical parameters change by ±25%. This shows the robustness and reliability of the controller when optimized by the proposed method in dynamic conditions. Thereby, the PO algorithm is proven to be one of the effective metaheuristic optimization methods for solving the LFC problem.

In the future, research will also expand the problem by considering the high penetration of renewable energy sources. The proposed method is combined with new optimization strategies for control, storage, and market operations to cope with the volatility and unpredictability of renewable energy. The application of advanced technologies such as artificial intelligence, deep learning, and big data in the LFC field is also a potential direction.

Conflict of Interest

The authors declare no conflict of interest.

Author Contributions

T. K. Do: Conceptualization, Methodology, Software, Writing - Original draft. T. L. Duong: Conceptualization Methodology, Revise & editing, Investigation, Supervision, Formal analysis.

Funding

No funding was received for this work.

Informed Consent Statement

Not applicable.

References

[1] Choudhary R., Rai J. N., and Arya Y., "Cascade FOPI-FOPTID controller with energy storage devices for AGC performance advancement of electric power systems," *Sustain. Energy Technol. Assessments*, Vol. 53, No. PC, p. 102671, 2022.

[2] Bevrani H., Golpîra H., Messina A. R, Hatziargyriou N., Milano F., and Ise T., "Power system frequency control: An updated review of current solutions and new challenges," *Electr. Power Syst. Res.*, Vol. 194, No. December 2020, 2021.

[3] Sharma D., "Load Frequency Control: A Literature Review," *Int. J. Sci. Technol. Res.*, Vol. 9, No. February, p. 2, 2020.

[4] Amiri F. and Moradi M. H., "Coordinated control of LFC and SMES in the power system using a new robust controller," *Iran. J. Electr. Electron. Eng.*, Vol. 17, No. 4, pp. 1–17, 2021.

[5] Khan I. A., Mokhlis H., Mansor N. N., Illias H. A., Jamilatul Awalin L., and Wang L., "New trends and future directions in load frequency control and flexible power system: A comprehensive review," *Alexandria Eng. J.*, Vol. 71, pp. 263–308, 2023.

[6] Rosaline A. D. and Somarajan U., "Structured H-Infinity controller for an uncertain deregulated power system," *IEEE Trans. Ind. Appl.*, Vol. 55, No. 1, pp. 892–906, 2019.

[7] Arya Y. and Kumar N., "Optimal control strategy–based AGC of electrical power systems: A comparative performance analysis," *Optim. Control Appl. Methods*, Vol. 38, No. 6, pp. 982–992, 2017.

[8] Zaheeruddin, Singh K., and Amir M., "Intelligent Fuzzy TIDF-II Controller for Load Frequency Control in Hybrid Energy System," *IETE Tech. Rev. (Institution Electron. Telecommun. Eng. India)*, Vol. 39, No. 6, pp. 1355–1371, 2022.

[9] Guo J., "The Load Frequency Control by Adaptive High Order Sliding Mode Control Strategy," *IEEE Access*, Vol. 10, pp. 25392–25399, 2022.

[10] Fernández-Guillamón A., Muljadi E., and Molina-García A., "Frequency control studies: A review of power system, conventional and renewable generation unit modeling," *Electr. Power Syst. Res.*, Vol. 211, No. January, p. 108191, 2022.

[11] Amir M., Zaery M., Singh K., Suhail Hussain S. M., and Abido M. A., "Enhancement of Frequency Regulation by TFOID Controller in Hybrid Renewable Energy with Battery Storage System Based Multi Area Microgrids," *IEEE Access*, Vol. PP, p. 1, 2024.

[12] Mohanty D. and Panda S., "Fractional order based controller for frequency control of hybrid power system," *1st IEEE Int. Conf. Sustain. Energy Technol. Syst. ICSETS 2019*, pp. 87–92, 2019.

[13] Kumar N., Tyagi B., and Kumar V., "Deregulated Multiarea AGC Scheme Using BBBC-FOPID Controller," *Arab. J. Sci. Eng.*, Vol. 42, No. 7, pp. 2641–2649, 2017.

[14] Saha A. and Saikia L. C., "Utilisation of ultra-capacitor in load frequency control under restructured STPP-thermal power systems using WOA optimised PIDN-FOPD controller," *IET Gener. Transm. Distrib.*, Vol. 11, No. 13, pp. 3318–3331, 2017.

[15] Priyadarshani S., Subhashini K. R., and Satapathy J. K., "Pathfinder algorithm optimized fractional order tilt-integral-derivative (FOTID) controller for automatic generation control of multi-source power system," Microsyst. Technol., Vol. 27, No. 1, pp. 23–35, 2021.

[16] Qu Z., Younis W., Liu X., Junejo A. K., Almutairi S. Z., and Wang P., "Optimized PID Controller for Load Frequency Control in Multi-Source and Dual-Area Power Systems Using PSO and GA Algorithms," IEEE Access, Vol. PP, p. 1, 2024.

[17] Ozumcan S., Ozturk A., Varan M., and Andic C., "A novel honey badger algorithm based load frequency controller design of a two-area system with renewable energy sources ☆," Energy Reports, Vol. 9, No. S12, pp. 272–279, 2023.

[18] Sharma A. and Singh N., "Load frequency control of connected multi-area multi-source power systems using energy storage and lyrebird optimization algorithm tuned PID controller," J. Energy Storage, Vol. 100, No. September, 2024.

[19] Daraz A., "Optimized cascaded controller for frequency stabilization of marine microgrid system," Appl. Energy, Vol. 350, No. July, p. 121774, 2023.

[20] Barakat M., "Novel chaos game optimization tuned-fractional-order PID fractional-order PI controller for load–frequency control of interconnected power systems," *Prot. Control Mod. Power Syst.*, Vol. 7, No. 1, 2022.

[21] Choudhary R., Rai J. N., and Arya Y., "FOPTID+1 controller with capacitive energy storage for AGC performance enrichment of multi-source electric power systems," *Electr. Power Syst. Res.*, Vol. 221, No. February, p. 109450, 2023.

[22] Swain N., Sinha N., and Behera S., "Stabilized frequency response of a microgrid using a two-degree-of-freedom controller with African vultures optimization algorithm," ISA Trans., Vol. 140, pp. 412–425, 2023.
[23] Guha D., Roy P. K., and Banerjee S., "A maiden application of salp swarm algorithm optimized cascade tilt-integral-derivative controller for load frequency control of power systems," *IET Gener. Transm. Distrib.*, Vol. 13, No. 7, p. 1110, 2018.
[24] Khamari D., Sahu R. K., Gorripotu T. S., and Panda S., "Automatic generation control of power system in deregulated environment using hybrid TLBO and pattern search technique," *Ain Shams Eng. J.*, Vol. 11, No. 3, pp. 553–573, 2020.
[25] Kennedy J., & Eberhart R., "Particle Swarm Optimization," Proceedings of ICNN'95-international conference on neural networks. Vol. 4, pp. 1942-1948, 1995.
[26] Abdel-Basset M., Mohamed R., and Abouhawwash M., "Crested Porcupine Optimizer: A new nature-inspired metaheuristic," Knowledge-Based Syst., Vol. 284, No. November 2023, p. 111257, 2024.
[27] Sowmya R., Premkumar M., and Jangir P., "Newton-Raphson-based optimizer: A new population-based metaheuristic algorithm for continuous optimization problems," Eng. Appl. Artif. Intell., Vol. 128, No. November 2023, p. 107532, 2024.
[28] Sharma J., Hote Y. V., and Prasad R., "PID controller design for interval load frequency control system with communication time delay," *Control Eng. Pract.*, Vol. 89, No. December 2018, pp. 154–168, 2019.
[29] Arya Y., "A novel CFFOPI-FOPID controller for AGC performance enhancement of single and multi-area electric power systems," *ISA Trans.*, Vol. 100, pp. 126–135, 2020.
[30] Jagatheesan K., Anand B., Samanta S., Dey N., Ashour A. S., and Balas V. E., "Particle swarm optimisation-based parameters optimisation of PID controller for load frequency control of multi-area reheat thermal power systems," *Int. J. Adv. Intell. Paradig.*, Vol. 9, No. 5–6, pp. 464–489, 2017.
[31] Abdollahzadeh B., Khodadadi N., Barshandeh S., Trojovsky P., Gharehchopogh F. S., El-kenawy E. M., Abualigah L., and Mirjalili S., *Puma optimizer (PO): a novel metaheuristic optimization algorithm and its application in machine learning*, Vol. 5. 2024.

T. K. Do received the B. Eng in Automation and Control Engineering Technology from the Industrial University of Ho Chi Minh City, Ho Chi Minh City, Vietnam, in 2023. Currently, he is pursuing a Master's degree at the Industrial University of Ho Chi Minh City, Ho Chi Minh City, Vietnam. His areas of interest are power system control, load frequency control, and heuristic optimization in power system control.

T. L. Duong received the B.Eng and M.Eng degrees in electrical engineering from the University of Technical Education Ho Chi Minh City, Vietnam, in 2003 and 2005, respectively. In 2014, he received the Ph.D. degree in electrical engineering from Hunan University, China. Currently, he is a Vice Dean at the Faculty of Electrical Engineering Technology, Industrial University of Ho Chi Minh City, Ho Chi Minh City, Vietnam. His research interests include power system operation, power system optimization, FACTS, optimization algorithms, and stability.